Lysozyme protected Cu Nano-Cluster: A Photo Switch for the Selective Sensing of Iron (Fe^{2+})

Anna Sebastian[‡1], *Aarya*[‡1], *Bibhu Ranjan Sarangi*[2,3] *and Supratik Sen Mojumdar**[1]

[1]Department of Chemistry, Indian Institute of Technology Palakkad, Kerala, India – 678 557
[2]Department of Physics, Indian Institute of Technology Palakkad, Kerala, India – 678 557
[3]Department of Biological Sciences and Engineering, Indian Institute of Technology Palakkad, Kerala, India – 678 557

Abstract

Protein capped metal nanoclusters gained a lot of recent attention due to their wide range of applications. However copper nanoclusters are difficult to synthesize due to their tendency to undergo oxidation. Here we successfully synthesized a stable, biocompatible lysozyme protected Cu nanocluster (Lys-Cu NC) using an optimized green one-pot protocol under aqueous condition at room temperature. The nanocluster showed a strong photoluminescence intensity (λ_{ex} = 365 nm, λ_{em} = 430 nm) which can be significantly and selectively quenched (off) by Fe^{2+} ions. Upon addition of NaOH the initial photoluminescence intensity can be recovered completely (on) thereby making the nanocluster a suitable candidate for a photo switch that can be reliably reused for the selective and sensitive detection of Fe^{2+} ions in the nanomolar (detection limit ~2.5 nM) concentration range. The synthesized nanocluster further has been successfully used to rapidly estimate iron level in complex systems (such as ground water and human hemoglobin samples). The photoluminescence intensity of the nanocluster is also sensitive towards temperature indicating that it can be used as a temperature sensor in different biological systems. This biofriendly nanocluster further used as an excellent nanoprobe for in-vivo cell imaging studies. Thus this Lys-Cu NC can be emerged as a next generation novel nanoprobe for various interdisciplinary applications.

*Email: supratik@iitpkd.ac.in

‡ These authors contributed equally.

INTRODUCTION

Metal nanoclusters (MNC) recently gained a lot of interest due to its wide range of applications in various interdisciplinary fields like optics, electronics, sensing, bio-medicine and catalysis.[1–4] They are ultra-small nanoparticles comprising of roughly ten to hundreds of atoms, with metal core size in the range of Fermi-wavelength of electrons (<2 nm).[2,5,6] The unique optical, electronic and chemical properties of metal nanoclusters compared to metal nanoparticles arise due to the presence of electronic transitions occurring between discrete energy levels.[2,5,6] Owing to the remarkable characteristics like strong fluorescence, high photostability, better water solubility, low toxicity, luminescent metal nanoclusters could serve as next generation fluorescent nanoprobes substituting the toxic quantum dots.[7,8] Incorporation of templates like proteins,[1,3,9–14] peptides,[15–19] polymers,[20–25] DNA[26–31] etc. could serve as stabilizing and reducing agents to enhance the structural stability, biocompatibility as well as photoluminescent property of the nanoclusters.

Among the various templates used for the synthesis of metal nanoclusters, protein-coated metal nanoclusters have emerged as a potential tool for several analytical and therapeutic applications namely sensing of cancer biomarkers, immunoassays, neurotransmitters, pharmaceutical compounds etc.[1,3,9–14] The presence of different amino acid residues with functional groups like -NH_2, -COOH, -OH and -SH in the side chains promote the stabilization of nanoclusters by coordinating with the metal ions.[10,32,33] The physicochemical properties of the protein-MNC can be tuned by varying the metal composition, size of the metal core, type of capping ligand, nature and concentration of reducing agents, reaction conditions etc.[32,34,35] Gold (Au)[7,11,14–16,36–43] and silver (Ag)[13,44–48] nanoclusters have extensively been explored among the various protein-protected noble metal nanoclusters. Due to their redox properties, Au and Ag were relatively easier to stabilize using the protein template.[10] However, in spite of being low-cost, more abundant and member of the same group in the periodic table, copper (Cu) NCs were less explored, mostly due to its low stability. Due to its high oxidation potential, copper is prone to oxidation and thus it has been challenging to stabilize copper NCs in aqueous medium.[20,32,49] Since copper is one of the most important constituents of the metalloproteins and biologically important metal, it was necessary to optimize the synthesis of Cu-NCs.

Recently researchers started to overcome the challenges and synthesized stable biocompatible Cu-NCs using various functional capping agents.[8,10,12,32,33,49–54] Compared to other proteins, Lysozyme (M.W. 14.3 kDa) is less expensive, commercially available, exhibits antibacterial property, high pH stability (isoelectric point ~11)[55,56] and strong binding affinity towards metal ions due to the presence of large number of (~56% of the total sequence) reactive side chains (-NH_2, -OH, -SH, -COOH),[57] making it a suitable capping agent for the synthesis of Cu NCs, but it has not been well explored.[12,52,53] Changing the

protein scaffold and reaction conditions can change the properties and applications of the NCs significantly.[1,20,58] Thus there are plenty of opportunities to explore the applications of the Lys-Cu NCs.

The limited number of reports on Lys-Cu NC mostly focused on its role as an cell imaging probe, but the metal sensing ability still remains unexplored.[12,52,53] Many metal ions in our biological system have been linked to a number of diseases.[59–61] Thus sensitive and selective detection of biologically relevant metal ions at a very low concentration range (~nM range) has extremely important therapeutic implications.[61–63] Iron is one of the most important and abundant constituent of the metalloproteins playing a crucial role in the enzymatic activity such as oxygen transport, electron transfer and other metabolic functions.[63–66] Iron imbalance in the physiological system can cause serious health issues and therefore it is absolutely necessary to quantify iron in the biological systems to diagnose any health problem.[66–68] In human, heme iron exists in +2 oxidation state.[66,69] Hemoglobin is the most important respiratory protein present in the red blood cell that carries oxygen from lung to the organs and tissues and transport back CO_2 from the tissues to the lung, thereby maintain oxygen level in our body. Fe^{2+} plays a key role in this oxygen transport process.[66,69] Anemia is a very common health problem caused by iron deficiency. Due to lack of Fe^{2+} ions, inadequate amount of oxygen being transported to the tissues that can make a person feel weak and tired.[66–68] In children iron deficient anemia can affect the growth and motor development.[66–68] Too much accumulation of iron in organs and tissues can also leads to diabetes, heart diseases, even neurodegenerative diseases.[66–68] Consumption of water containing more than 0.3 mg/L of iron (Fe^{2+}/Fe^{3+}) is also considered to be a threat to human health.[70] Thus it is utmost important to accurately quantify Fe^{2+} in human body as well as other complex systems such as ground water.

Although, several protocols were reported for the synthesis of protein-coated Cu-NCs, majority of them suffered from the drawbacks such as, requirement of reducing agents, expensive biofriendly templates and/or harsh reaction conditions. Here, we report a green and efficient protocol for the one-pot synthesis of blue emitting Cu-NCs stabilized with Lys at room temperature and aqueous conditions in the absence of any reducing agent and characterized its spectroscopic properties. The synthesized Lys-Cu NCs showed photoluminescence properties with a significant quantum yield and high photostability with various interesting applications. The NC is biocompatible and can selectively detect Fe^{2+} ions in the nanomolar (as low as ~2.5 nM, i.e. 140 ng/L) concentration range in different complex systems. Fe^{2+} ions can significantly quench (~95%) the fluorescence signal which can be recovered completely by adding NaOH and thus the NC can be reused. The NC can further be used to detect Fe^{2+} even in complex systems such as human hemoglobin and different water samples. It can also be used as an excellent nanoprobe for cell-imaging. Upon further investigation we observed that the photoluminescence intensity is sensitive towards temperature and showed a systematic reversible behavior. Thus, it can also be used as a temperature sensor

within biological systems. Overall we present a concise study on the synthesis and application of the Lys-Cu NCs in this report with the plausible mechanistic insight of its photophysical behaviours.

MATERIALS AND METHODS :

Materials

Lysozyme from hen egg white was purchased from Sisco Research Laboratories Pvt. Ltd. (SRL). Copper Chloride ($CuCl_2.2H_2O$), and sodium hydroxide (NaOH) for the synthesis of Lys-Cu nanocluster (NC) were purchased from Nice Chemicals (NICE). To study the metal ion sensing the following salts of different metal ions were purchased either from SRL or, NICE: calcium chloride ($CaCl_2$), lead nitrate [$Pb(NO_3)_2$], mercuric chloride ($HgCl_2$), magnesium chloride ($MgCl_2$), nickel sulphate ($NiSO_4$) and zinc sulphate ($ZnSO_4$), cobalt nitrate [$Co(NO_3)_2$], chromic nitrate [$Cr(NO_3)_2$], ferrous chloride ($FeCl_2$), ferric chloride ($FeCl_3$), manganese chloride ($MnCl_2$), potassium chloride (KCl) and sodium chloride (NaCl). Zn powder was purchased from Nice Chemicals. Quinine hemi-sulfate dye and hemoglobin (human) lyophilized powder were purchased from sigma-aldrich. L-ascorbic acid was purchased from Sisco Research Laboratories Pvt. Ltd. (SRL). All solutions were prepared using double distilled water from Biopak Polisher Milli-Q water system (CDUFBI001). All the reagents were used as received without further purification.

Synthesis of photoluminescent copper nanocluster

Lysozyme protected Cu nanocluster (Lys-Cu NC) was prepared in a molar ratio of 1:1 under aqueous condition following the previously reported method with some modifications.[12,53] Initially, 20 mg of lysozyme (10 mg/ml) was dissolved in 2 ml of Milli-Q water and 1 ml of $CuCl_2$ was added from 1.4 mM stock solution. The reaction mixture was stirred at 40° C for half an hour. To this solution 100 µl of 1 M NaOH was added dropwise in regular intervals to adjust the pH ~12. Initially upon addition of NaOH the colour of the solution changed from colourless to turbid white and ultimately to transparent pale violet on further addition of NaOH. The solution kept under vigorous stirring at room temperature for ~ 24 h (Scheme 1). After completion of the reaction the solution was centrifuged (at 14,000 x g for 5 mins) and the supernatant was collected and stored at 4^0C under dark condition for further use.

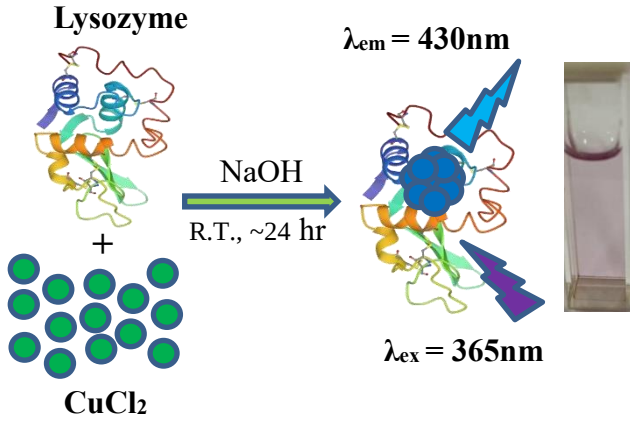

Scheme 1: Schematic representation of the synthesis of lysozyme protected Cu nanocluster. Crystal structure of lysozyme is taken from ref 86 (PDB ID: 6LYZ).

Instrumentation

Absorbance measurements were recorded using Thermo Scientific (Evolution 201) UV-Visible Spectrophotometer. Steady state photoluminescence studies were performed on Perkin Elmer Fluorescence Spectrometer (FL 8500). The Lys-Cu nanocluster solution was excited at 365 nm and the spectra was scanned from 390 nm to 650 nm at a speed of 240 nm min^{-1} keeping the excitation and emission slits at 5 nm. Temperature dependent emission studies were done on a Horiba Jobin Yvon Fluorolog 3-111 instrument. For monitoring the lifetime of Lys-Cu NC, time resolved fluorescence measurements were carried out using a DeltaFlex Time Correlated Single Photon Counting (TCSPC) spectrometer with a hybrid photomultipler detector. The second harmonic output of a tunable Mai-Tai Laser was used as an excitation source (λ_{ex} = 365 nm) with a repetition rate of 8 MHz. The full width at half-maxima (FWHM) of the Instrument Response Function (IRF) was 73 ps. To avoid anisotropic effects the decays were collected at magic angle (54.7°) with respect to vertically polarized excitation light. To characterize the size of the nanoclusters, Transmission Electron Microscopy (TEM) [FEI TALOS 200 (field-emission electron microscope)] operating at 200 kV was used. The sample was drop casted on a carbon coated copper grid. Centrifugation was done using a non-refrigerated centrifuge from Dinesh Scientific (Model No: DS-NRC-473). The photoluminescence quantum yield (ϕ) of the synthesized nanocluster was measured using the equation:[71]

$$\phi_s = \phi_{ref} \frac{I_s}{I_{ref}} \frac{A_{ref}}{A_s} \frac{n_s^2}{n_{ref}^2}$$

where, ϕ, I, A and n denote the quantum yield, integrated emission intensity, absorbance and refractive index of the medium respectively. The suffix 's' stands for sample and 'ref' stands for reference. Quinine sulfate (ϕ = 0.546)[72] was used as a reference in our study.

Metal sensing Studies

To study the metal ion sensing Lys-Cu nanocluster solution was incubated with desired concentration of different metal ions for ~3 mins prior to the measurement. To check the sensitivity of Fe^{2+} ion detection, different concentrations of Fe^{2+} ions (from 1 nM to 1 mM) were gradually added to the same volume of Lys-Cu NC and the PL intensity was measured after each addition. The limit of detection was determined using the formula, Limit of Detection (LOD) = $\frac{3\sigma}{K}$, where σ is the standard deviation and K is the slope of the straight line obtained from the plot.[73,74]

Cell Viability and Imaging:

For cell viability and imaging studies the Lys-Cu NC sample was washed thoroughly using a spin filter (Amicon^{R} Ultra 10 K) to adjust the pH to 7.5. The cell viability study of the Lys-Cu nanocluster was carried out on 3T3 (normal mouse fibroblast) cells using MTT assay which measures cellular metabolic activity as an indicator of cell viability. The cells were cultured in Dulbecco's Modified Eagle Medium (DMEM) high glucose media (Himedia) with 10% Fetal bovine serum (FBS) (Himedia), 1% Penstrep, 0.2% of Amphotericin (Gibco Life Tech), 1% antibiotic at 37 ^{0}C and 5% CO_2. For viability study, the cells were seeded in 96 well plate at 1 x 10^4 cells per well and allowed to adhere to the substrate with overnight incubation. The cells were incubated with Lys-Cu nanocluster at variety of concentration with minimum of 9 µg/ml and maximum of 2.88 mg/ml for 24 hours. Post incubation 10 µl of MTT was added to each well with final concentration of 0.5 mg/ml. The formazan crystals formed were dissolved in DMSO and absorbance was recorded in a plate reader (Biotech Epoch 2NS Gen5) at 590 nm using a 620 nm reference filter. For cell imaging the cells were incubated with Lys-Cu nanocluster at 20 µm concentration for 3 hours. Imaging was done using Epifluorescence microscope (Olympus IX83) with suitable fluorescence filters.

RESULTS AND DISCUSSIONS

Lysozyme protected Cu NC shows photoluminescence properties:

The Lys-Cu NC showed a strong photoluminescence intensity (λ_{ex} = 430 nm) when excited at 365 nm with a significant quantum yield (ϕ = 0.133) (Figure 1). Upon comparing the emission intensity with that of pure protein, we concluded that the luminescent properties are inherent characteristics of the NC stabilized by Lys (Figure S1). Based on the emission maxima, the number of metal atoms present in the NC can be theoretically predicted reliably using the Jellium Model [$E_{NC} = E_f/(N)^{1/3}$, where E_{NC} is the emission energy of the NC corresponding to the emission maxima, E_f is the Fermi energy of the metal in bulk and N is the number of atoms in the NC][75,76] which matches nicely with the experimental data obtained from MALDI (Matrix Assisted Laser Desorption/Ionization) mass spectra.[49,63,76] According to this model, emission peak around 430 nm for Lys-Cu NC indicates the presence of Cu_{14} in the NC. The ultrasmall size (average size ~2 nm) of Lys-Cu NC is confirmed from the transmission electron microscope (TEM) image (Figure S2).

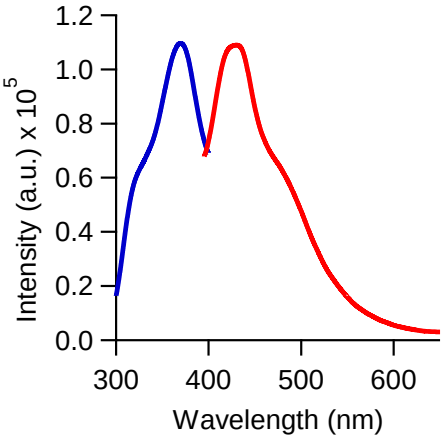

Figure 1. Excitation (λ_{em} = 430 nm) (–) and emission spectra (λ_{ex} = 365 nm) (–) of Lys-Cu NC.

Initially the amino acid residues present in the protein scaffold stabilizes the Cu^{2+} ions via electrostatic interaction. At an optimum pH ~12, the amino acid residues reduce Cu^{2+} ions to Cu^0.[12,52,53] Previous x-ray photoelectron spectroscopy (XPS) studies confirmed that Cu mostly remains as Cu^0 in the lysozyme protected Cu nanoclusters.[12,52,53] From the time resolved spectroscopic analysis, the photoluminescent lifetime of Cu-Lys NC was found to be 3.9 ns (Figure S3). The high photostability of Lys-Cu NC were confirmed by a complete retention of its photoluminescent properties for over a month when stored at 4°C (Figure S4). In general oxidizing agents like H_2O_2 can easily oxidize the protein protected Cu nanoclusters thereby quench the photoluminescence intensity.[10,49] In the case of Lys-Cu NC, absolutely no quenching effect has been observed in the presence of H_2O_2 (Figure S5) suggesting that the NC is resistant towards oxidative damage.

Selective and sensitive sensing of Fe^{2+}:

In this report an assay based on the quenching of the luminescence intensity of the Lys-Cu NC was developed to rapidly detect the Fe^{2+} ions in aqueous medium with high selectivity and sensitivity. Fe^{2+} (500 μM) can significantly quench (~85%) the photoluminescence intensity of the NC (Figure 2). To check the selectivity of Fe^{2+}, same concentration (500 μM) of a series of other metal ions were added respectively to the Lys-Cu NC solution. The quenching efficiency of the other metal ions were significantly lower than that of the Fe^{2+} ions (Figure 3) thus indicating a selective detection of Fe^{2+}. Though Fe^{3+} ions show relatively higher quenching efficiency (~ 38%) compared to other metal ions, it is substantially less than that of Fe^{2+} ions (~ 85%)

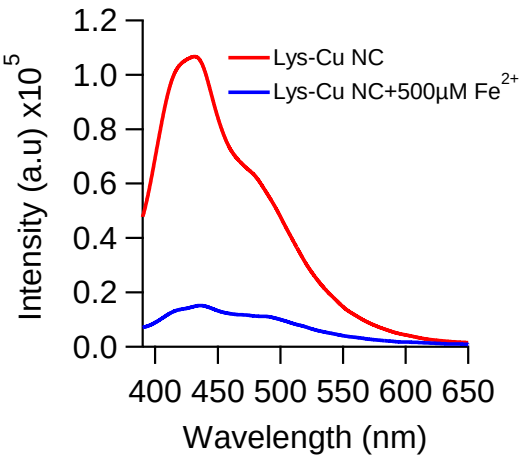

Figure 2. Emission spectra (λ_{ex} = 365 nm) of Lys-Cu NC in the absence (–) and presence of 500 μM Fe^{2+} ions (–).

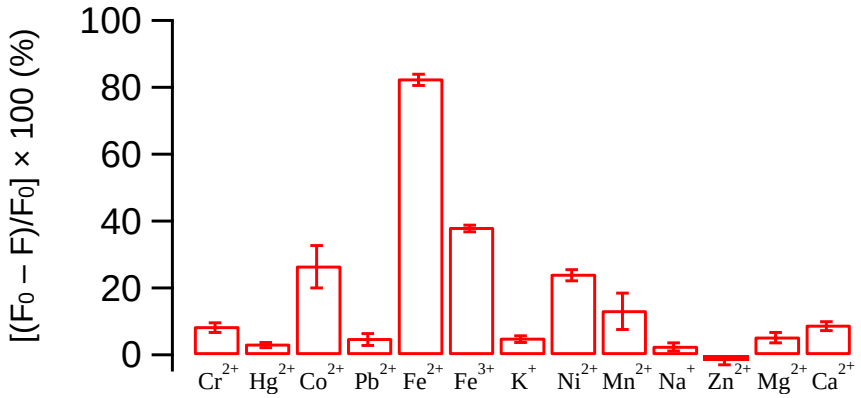

Figure 3. Quenching (%) of Lys-Cu NC photoluminescence by different metal ions (500 μM). F_0 and F represent the photoluminescence intensities in the absence and presence of metal ions respectively.

(Figure 3), not affecting the selectivity of Fe^{2+}. In aqueous solution, Fe^{2+} readily oxidizes to Fe^{3+} making it challenging to differentiate Fe^{2+} from Fe^{3+} and selectively detect only Fe^{2+}. Using Lys-Cu NC we could overcome this challenge by differentiating Fe^{2+} from Fe^{3+} and selectively detecting Fe^{2+} only in aqueous solution.

Quenching of fluorescence intensity by metal ions mainly occur due to the photoinduced electron/charge transfer transition between the fluorophore and the metal ions.[45,63,71,77] However, it is extremely difficult to identify the direction of the electron transfer process.[45,63,71,77] This quenching process can either be static or, dynamic in nature.[45,63,71,77] The synthesized NC was extremely resistant towards oxidation (Figure S5) clearly showing its inability to transfer an electron to the metal ions. On the other hand Fe^{2+} (d^6) ions have a very strong tendency to oxidize by giving up one electron easily to attain a more stable [Fe^{3+}(d^5)] electronic configuration. Based on this we can predict that the electron transfer is occurring from Fe^{2+} to the nanocluster.

To test the sensitivity, different concentrations of Fe^{2+} ions (1 nM to 1 mM) were added gradually to the Lys-Cu NC solution. As a result the PL intensity gradually decreased with increasing Fe^{2+} concentration (Figure S6). At around 1 mM Fe^{2+} the PL intensity is quenched by ~95% (Figure S6). To confirm that the quenching of the PL intensity is due to the interaction between Cu NC & Fe^{2+} ions and not due to the interaction between the protein & metal ions, same concentrations of Fe^{2+} ions were added to an aquoeus solution of Lysozyme (~ 0.7 mM). Lysozyme exhibits a very weak emission intensity when excited at 365 nm. Upon addition of 1mM Fe^{2+}, no significant quenching of the fluorescence intensity of the protein was observed confirming an interaction between the Fe^{2+} and the Cu NC (Figure S7). Hence it could be concluded that Cu NC are solely responsible for the metal sensing activity. The limit of detection (LOD) for Fe^{2+} ions was calculated to be 2.5 nM (i.e. ~ 140 ng/L). Thus

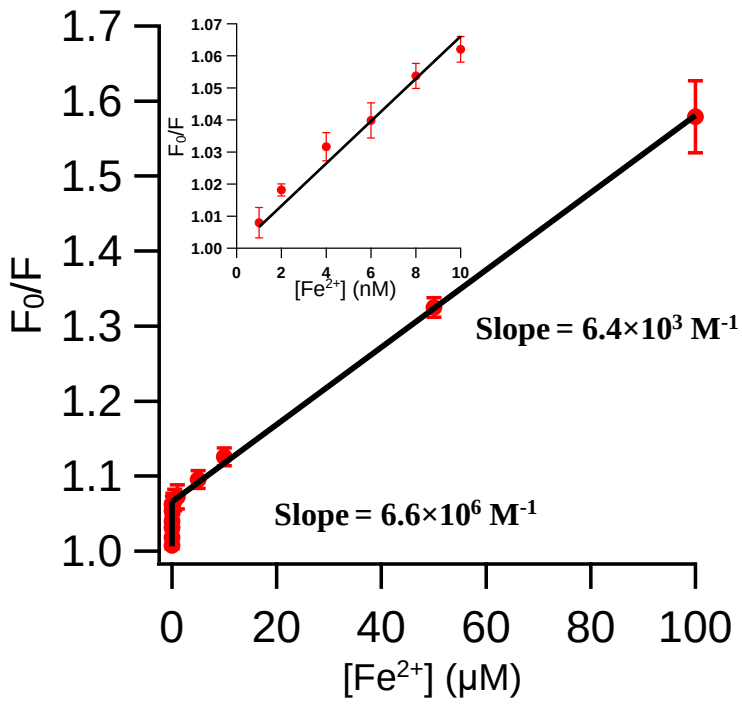

Figure 4: Stern-Volmer plot corresponding to the quenching of Lys-Cu NC photoluminescence intensity by gradual addition of Fe^{2+} ions. The black line represents linear fit. Inset captures the initial part (up to 10 nM Fe^{2+}) of the plot.

the so-synthesized nanocluster can be applied for the selective and ultra-sensitive detection of Fe^{2+} in the nano-molar concentration range.

The Stern-Volmer plot (F_0/F vs concentration of the quencher (Fe^{2+}), where F_0 and F are the photoluminescence intensities in the absence and presence of quencher respectively) showed a two step quenching process (deviate from the typical linear Stern-Volmer plot with one slope) indicating a more complex quenching process involving different kinetics which depends upon the concentration of the quencher (Figure 4). Initially the photoluminescence intensity changed very rapidly up to ~10 nM with a Stern-Volmer constant (K_{SV}) of ~6.6×10^6 M^{-1}. After 10 nM, the quenching process slowed down and can be fitted with a different straight line (Slope ~ 6.4×10^3 M^{-1}, intercept ~1.06). Most commonly Stern -Volmer plot deviates from linearity with an upward curvature due to the presence of both static and dynamic quenching mechanism.[71,78] Pure dynamic/collisional quenching can also lead to a non-linear Stern-Volmer plot but with downward curvature in some extreme/rare cases if some fluorophores are less accessible than others.[79,80] For this later case a modified Stern-Volmer plot [$F_0/(F_0 - F)$ vs 1/[Q]] should results in a linear plot[71,80] which could not be seen in the present case (Figure S8). In our case we could see a very interesting sharp transition at ~10 nM which has not been seen earlier.[45,63,81] The initial high slope indicating the existence of static quenching as the kinetics can not be explained with diffusion controlled quenching only.[80] Involvment of static quenching is further confirmed by lifetime measurements. In static quenching a complex is formed at the ground state between the fluorophore and the quencher which does not affect the lifetime of the system.[63,71,82] On the other hand no such complex is formed for the dynamic/collisional quenching which results in a significant quenching of the lifetime of the fluorophore.[63,71,77,82] The lifetime of the Lys-Cu NC did not change upon addition of Fe^{2+} ions (Figure S9), clearly suggesting that the quenching process is purely static in nature. The difference in the slope may be attributed to the difference in availability of the binding sites on the surface of the nanocluster. Initially at a very low Fe^{2+} concentration (~10 nM) the ions can easily bind to the surface of the nanocluster leading to a complex formation followed by a very fast static quenching. Above ~10 nM the complex formation slows down (may be due to some steric hindrance between the scaffold surface and the metal ions) leading to a slower quenching process. Overall the quenching process for this system is extremely complex and further study is required to elucidate the exact mechanistic details.

When aqueous solution of Fe^{2+}/Fe^{3+} ions are treated with NaOH, corresponding hydroxide salts precipitate out from the solution.[83] Using this technique we removed the Fe^{2+} ions from the Lys-Cu NC solution and check its reusability. The quenched Lys-Cu NC in the presence of 1 mM Fe^{2+} was treated with 1M NaOH (~100 μL) and the precipitate was separated from the supernatant using centrifugation. Remarkably, the supernatant containing the Lys-Cu NC showed high photoluminescence intensity with ~100% recovery of the initial intensity (Figure S10). The initial PL intensity can be retained even after at

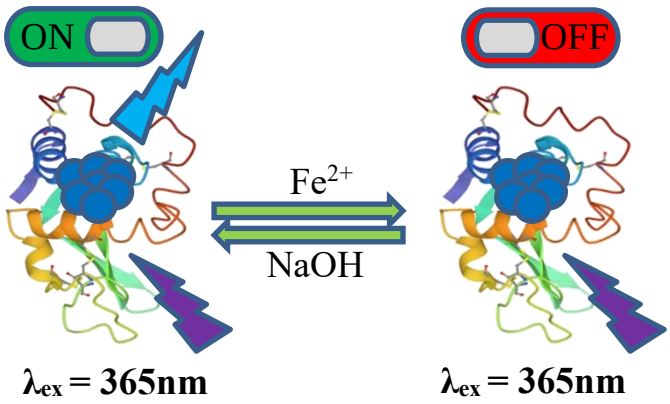

Scheme 2: Photoluminescence intensity quenched by Fe^{2+} ions can be recovered completely by treating the sample with 1M NaOH thus can be used as a photo switch.

least 4 quenching cycles (Figure S10). Thus Lys-Cu NC can be reliably used as a robust reusable photo switch to turn on/off the metal sensor using NaOH/Fe^{2+} respectively (Scheme 2).

Quantification of Fe^{2+} in complex systems using Lys-Cu NC:

We extended our sensing studies to check the applicability of the Lys-Cu NC as a Fe^{2+} sensor in real complex samples. We investigated the level of Fe^{2+} in water samples collected from different practical sources. We treated the water samples with Zn powder to convert the oxidized Fe^{3+} ions (if any) to Fe^{2+} ions. The water sample collected from a nearby pond contains high level (~6.43 mg/L) of Fe^{2+} (Figure S11 and Table 1) which is higher than the acceptable level (<0.3 mg/L),[70] indicates that the water is contaminated and consumption of this water may cause health issues. On the other hand water sample collected from the well contains ~0.3 mg/L Fe^{2+} which is just around the acceptable level. Water collected from the water purifier (that uses reverse osmosis technique) contains very low level of iron (~0.0052 mg/L), well below the allowed range, thus safe to drink.

To check the accuracy of our method, we used a sample of known concentration of Hemoglobin (human). Hemoglobin gets readily oxidized in air and thus mostly remains as methemoglobin. Ascorbic acid has been used as an effective drug to treat methemoglobinemia to convert methemoglobin (containing Fe^{3+}) to hemoglobin (containing Fe^{2+}).[84,85] Thus we added ~ 500 μM (~90 μg/ml) ascorbic acid to the hemoglobin solution to reduce the Fe^{3+} (if any) to Fe^{2+}. We added ~20 μg/ml (i.e. ~ 0.3 μM) of hemoglobin (human) to the Lys-Cu NC and observed ~7% quenching of the PL intensity (Figure S12) which corresponds to ~1.32 uM (~74 ng/ml) Fe^{2+} ions (estimated from the Stern-Volmer plot, Figure 4). Each hemoglobin molecule contains 4 Fe^{2+} ions and the percentage of iron in human hemoglobin is ~0.34%.[86] Thus 20 μg/ml (~ 0.3 μM) hemoglobin should contain ~ 68 ng/ml (~1.2 μM) Fe^{2+} ions. Thus, theoretically estimated value of Fe^{2+} (~68 ng/ml) in hemoglobin solution remarkably matched (>90%) with our experimentally obtained value (~74 ng/ml) (Figure S12). The results thus suggests that our method is extremely robust and reliable, we can use the synthesized Lys-Cu NC for the rapid and accurate quantification of iron in any biologically (eg. blood samples) or environmentally (water samples) relevant complex systems.

Table 1: Level of iron in different water samples.

Water Source	Amount of Fe^{2+} (mg/L)
Pond	6.43 ± 1.6
Well	0.3 ± 0.1
Water Purifier	0.0052 ± 0.0004

Temperature Dependent Photoluminescence Property of the NC:

Another interesting application of the Lys-Cu NC is temperature sensing. The photoluminescence intensity of the Lys-Cu NC is extremely sensitive towards temperature, hence can be used as an temperature sensor for different biological systems. With gradual increase in temperature (from 20 ^{0}C to 60 ^{0}C) the PL intensity of the Lys-Cu NC decreases while in the reverse process (from 60 ^{0}C to 20 ^{0}C) the intensity gradually

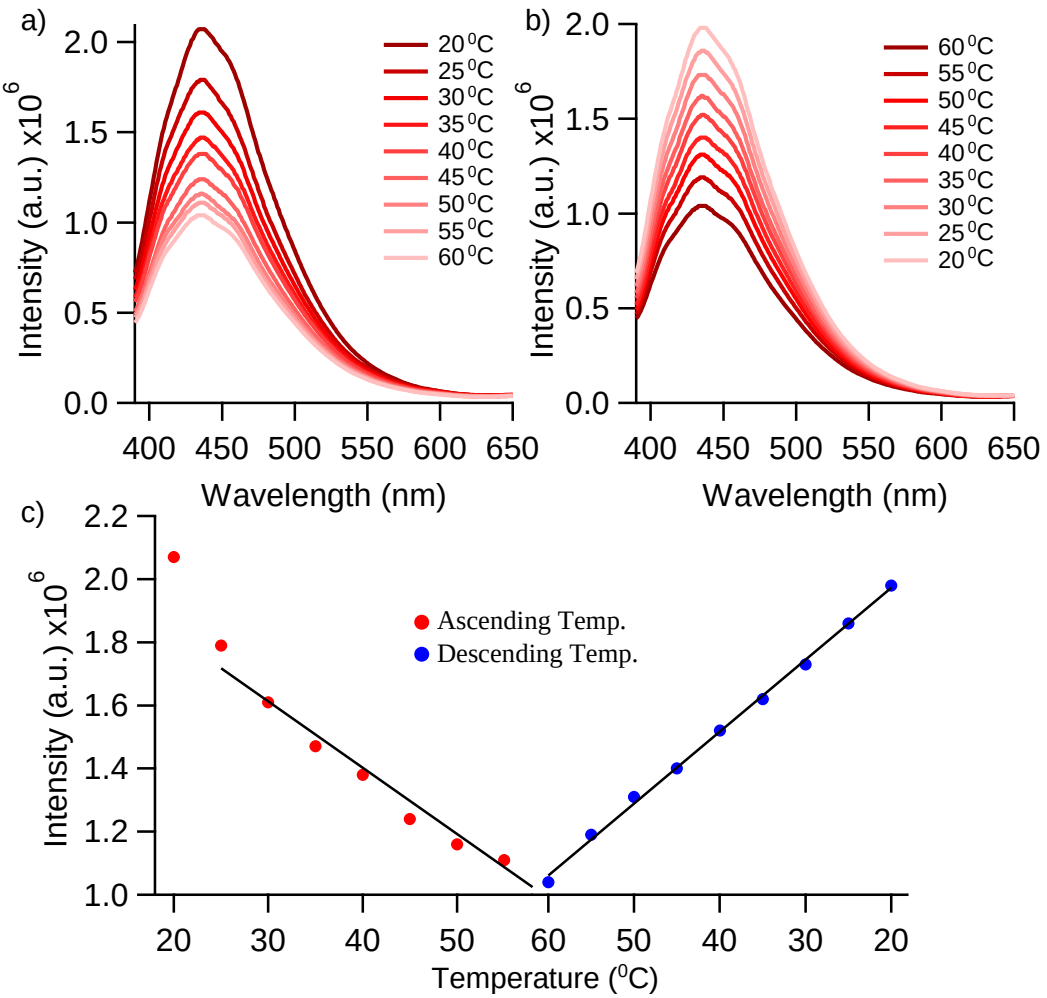

Figure 5 Variation in photoluminescence intensity with temperature a) ascending from 20-60 ^{0}C and b) descending from 60-20 ^{0}C c) Plot of PL Intensity of Cu-Lys NC as a function of temperature shows reversibility.

increases and can be restored completely at ~20 ^{0}C (Figure 5a,b). This process is reversible and can be repeated for several cycles without changing its PL properties (Figure S13). Lysozyme is quite stable against thermal denaturation, it can exist even at 55 ^{0}C for about an hour without much denaturation, only above 60 ^{0}C it starts to denature completely .[87,88] Thus, during the increase in temperature the protein scaffold partially unfolds[89] exposing the NC towards the polar solvent thereby decreasing the PL intensity.[10] Opposite trend can be seen during the gradual decrease in the temperature as the protein scaffold refolds back to its native structure. Most interestingly this reversible process (PL intensity vs temperature plot) is linear in nature and occurs without any change in the PL property of the NC suggests that some contacts still keep the NC in its original position (without any disintegration) even at a high temperature (~60 ^{0}C) (Figure 5c, S14). During refolding the protein scaffold follows the same pathway (crossing the same set of energy barriers) restoring the same set of contacts that helps the NC recover its initial PL intensity. The linear dependency of the PL intensity on the temperature thus makes it a good candidate for an intracellular temperature sensor (nano-thermometer) for different biological systems.

Lys-Cu NC: An Excellent Nanoprobe for Cell Imaging:

The synthesized Lys-Cu NC showed excellent biocompatibility. The in-vitro toxicity study of the lysozyme stabilized copper nanocluster was demonstrated through MTT based cell viability assay. The viability of 3T3 fibroblast cells after treating with the nanocluster for an incubation period of 24 hr was studied as a function of their concentration. The nanocluster exhibited biocompatibility over a wide range of concentrations (Figure 6a). More than 50% viability was observed even at a very high concentration (~720 µg/ml) of the nanocluster, thereby confirms the non-cytotoxicity of the nanocluster indicating that the nanocluster is suitable for intracellular studies. Cell imaging studies using the synthesized Lys-Cu NC has

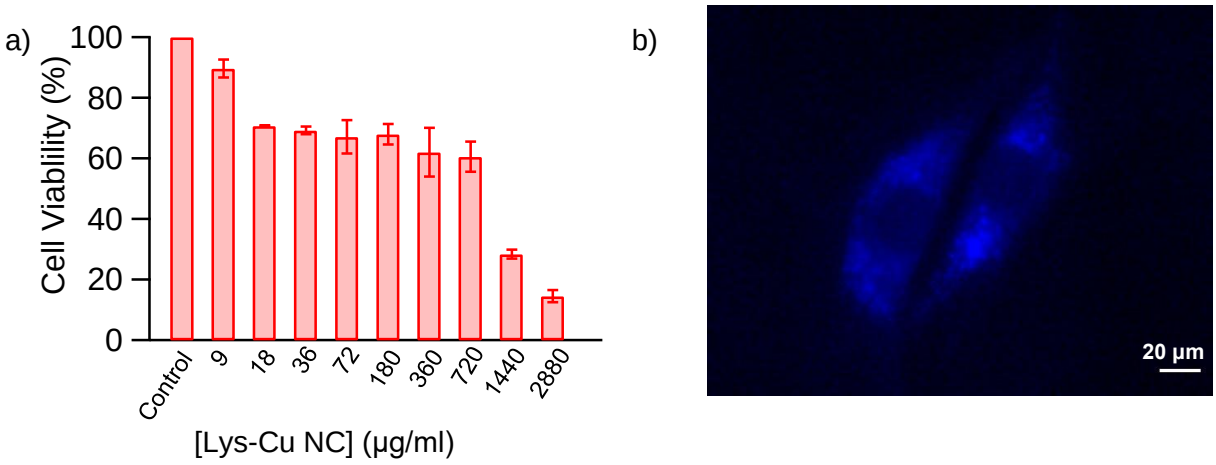

Figure 6 a) Cell viability assay showing the cytotoxicity of the nanocluster on 3T3 fibroblast cells. The nanocluster is non-toxic to the cells. b) Epifluorescence microscope image of 3T3 fibroblast cells incubated with Lys-Cu NC.

also been explored which suggests that the nanocluster can be used as an excellent nanoprobe for cell imaging. 3T3 fibroblast cells were incubated with 360 μg/ml of Lys-Cu NC for 3 hrs and the images were captured using a fluorescence microscope (Figure 6b). The image indicated that the nanocluster was mostly located at the cytosolic part of the cells. Thus the lysozyme stabilized Cu-NC synthesized through the reported protocol can be further used as an in-vivo biomarker and thereby apply in various fields of medical diagnosis and therapy.

CONCLUSIONS

In summary, we have successfully developed a green protocol for one-pot synthesis of Lys-Cu NC under ambient condition in the absence of any toxic reducing agents. The synthesized Lys-Cu NC showed photoluminescence properties with high quantum yield, photostability and biocompatibility. This NC can be re-used for the rapid, sensitive and selective detection of Fe^{2+} ions in the sub nanomolar concentration range (~2.5 nM, i.e. 140 ng/L). Iron level in many complex system (such as ground water and hemoglobin) can also be estimated reliably and rapidly using this nanocluster suggesting its practical applicability as an iron sensor in blood and other biologically and environmentally relevant samples. The cell imaging and viability studies indicated that our NC is nontoxic and showed excellent biocompatibility making it an ideal candidate for the next-generation nano-sensor. The temperature dependent PL reversibility exhibited by the NC proved themselves to be a potential candidate for an in-vivo temperature sensor. Overall our concise results showed that these novel NCs can open up promising avenues in the interdisciplinary area of bio-sensing, drug-delivery, diagnostic and therapeutic applications.

AUTHOR INFORMATION AND CNTRIBUTION

Corresponding Author

Supratik Sen Mojumdar- Department of Chemistry, Indian Institute of Technology Palakkad, Kerala, India – 678 557; Email: supratik@iitpkd.ac.in

Authors

Anna Sebastian- Department of Chemistry, Indian Institute of Technology Palakkad, Kerala, India – 678 557

Aarya- Department of Chemistry, Indian Institute of Technology Palakkad, Kerala, India – 678 557

Bibhu Ranjan Sarangi- Department of Physics and Department of Biological Sciences & Engineering, Indian Institute of Technology Palakkad, Kerala, India – 678 557

Author Contributions

‡ These authors contributed equally.

CONFLICTS OF INTERESTS

There are no conflicts to declare.

ACKNOWLEDGEMENTS

S.S.M. thanks SERB, Government of India (Project no. SRG/2020/001710) and IIT Palakkad for financial assistance. B.R.S thanks SERB, Government of India (Project no. ECR/2016/001986) for financial support. A.S. thanks CSIR and A. thanks UGC, Government of India for providing fellowships. S.S.M thanks Time Resolved Fluorescence Spectroscopy and Microscopy facility, IIT Bombay for lifetime measurements and FIST facility, IISER Bhopal for TEM measurement. The authors thank Mr. Saurabh Rai, IISER Bhopal for helping with the temperature dependent steady state emission and TEM measurements.

REFERENCES

1 I. Zare, D. M. Chevrier, A. Cifuentes-Rius, N. Moradi, Y. Xianyu, S. Ghosh, L. Trapiella-Alfonso, Y. Tian, A. Shourangiz-Haghighi, S. Mukherjee, K. Fan and M. R. Hamblin, *Mater. Today*, , DOI:10.1016/j.mattod.2020.10.027.
2 Z. Lin, N. Goswami, T. Xue, O. J. H. Chai, H. Xu, Y. Liu, Y. Su and J. Xie, *Adv. Funct. Mater.*, 2021, **31**, 2105662.
3 X. Meng, I. Zare, X. Yan and K. Fan, *WIREs Nanomedicine Nanobiotechnology*, 2020, **12**, e1602.
4 L. Shang, J. Xu and G. U. Nienhaus, *Nano Today*, 2019, **28**, 100767.
5 Y. Lu and W. Chen, *Chem. Soc. Rev.*, 2012, **41**, 3594–3623.
6 J. P. Wilcoxon and B. L. Abrams, *Chem. Soc. Rev.*, 2006, **35**, 1162–1194.
7 C.-A. J. Lin, T.-Y. Yang, C.-H. Lee, S. H. Huang, R. A. Sperling, M. Zanella, J. K. Li, J.-L. Shen, H.-H. Wang, H.-I. Yeh, W. J. Parak and W. H. Chang, *ACS Nano*, 2009, **3**, 395–401.
8 W.-F. Lai, W.-T. Wong and A. L. Rogach, *Adv. Mater.*, 2020, **32**, 1906872.
9 P. L. Xavier, K. Chaudhari, A. Baksi and T. Pradeep, *Nano Rev.*, 2012, **3**, 10.3402/nano.v3i0.14767.
10 S. Ghosh, N. K. Das, U. Anand and S. Mukherjee, *J. Phys. Chem. Lett.*, 2015, **6**, 1293–1298.
11 S. Chattoraj and K. Bhattacharyya, *J. Phys. Chem. C*, 2014, **118**, 22339–22346.
12 R. Ghosh, A. K. Sahoo, S. S. Ghosh, A. Paul and A. Chattopadhyay, *ACS Appl. Mater. Interfaces*, 2014, **6**, 3822–3828.
13 Z. Gao, F. Liu, R. Hu, M. Zhao and N. Shao, *RSC Adv.*, 2016, **6**, 66233–66241.
14 S. Chattoraj, M. A. Amin and K. Bhattacharyya, *Chemphyschem Eur. J. Chem. Phys. Phys. Chem.*, 2016, **17**, 2088–2095.
15 Y. Li, M. Yuan, A. J. Khan, L. Wang and F. Zhang, *Colloids Surf. Physicochem. Eng. Asp.*, 2019, **579**, 123666.
16 Q. Wen, Y. Gu, L.-J. Tang, R.-Q. Yu and J.-H. Jiang, *Anal. Chem.*, 2013, **85**, 11681–11685.
17 Y. Gu, Q. Wen, Y. Kuang, L. Tang and J. Jiang, *RSC Adv.*, 2014, **4**, 13753–13756.
18 W. Song, R.-P. Liang, Y. Wang, L. Zhang and J.-D. Qiu, *Chem. Commun.*, 2015, **51**, 10006–10009.
19 H. Huang, H. Li, A.-J. Wang, S.-X. Zhong, K.-M. Fang and J.-J. Feng, *Analyst*, 2014, **139**, 6536–6541.
20 A. Baghdasaryan and T. Bürgi, *Nanoscale*, 2021, **13**, 6283–6340.
21 Y. Li, L. Feng, W. Yan, I. Hussain, L. Su and B. Tan, *Nanoscale*, 2019, **11**, 1286–1294.
22 J. Benavides, I. Quijada-Garrido and O. García, *Nanoscale*, 2020, **12**, 944–955.
23 Y.-S. Lin, L.-W. Chuang, B.-Y. Wu, Y.-H. Lin and H.-T. Chang, *Sens. Actuators B Chem.*, 2021, **333**, 129356.
24 G. Qu, T. Jiang, T. Liu and X. Ma, *ACS Appl. Mater. Interfaces*, 2022, **14**, 2023–2028.

25 K. Dong, J. Zhou, T. Yang, S. Dai, H. Tan, Y. Chen, H. Pan, J. Chen, B. Audit, S. Zhang and J. Xu, *Appl. Spectrosc.*, 2018, **72**, 1645–1652.
26 J. T. Petty, J. Zheng, N. V. Hud and R. M. Dickson, *J. Am. Chem. Soc.*, 2004, **126**, 5207–5212.
27 S. Chakraborty, S. Babanova, R. C. Rocha, A. Desireddy, K. Artyushkova, A. E. Boncella, P. Atanassov and J. S. Martinez, *J. Am. Chem. Soc.*, 2015, **137**, 11678–11687.
28 G. Liu, Y. Shao, K. Ma, Q. Cui, F. Wu and S. Xu, *Gold Bull.*, 2012, **45**, 69–74.
29 Y. Chen, M. L. Phipps, J. H. Werner, S. Chakraborty and J. S. Martinez, *Acc. Chem. Res.*, 2018, **51**, 2756–2763.
30 L. Qi, Y. Huo, H. Wang, J. Zhang, F.-Q. Dang and Z.-Q. Zhang, *Anal. Chem.*, 2015, **87**, 11078–11083.
31 C. Song, J. Xu, Y. Chen, L. Zhang, Y. Lu and Z. Qing, *Molecules*, 2019, **24**, 4189.
32 S. Shahsavari, S. Hadian-Ghazvini, F. H. Saboor, I. M. Oskouie, M. Hasany, A. Simchi and A. L. Rogach, *Mater. Chem. Front.*, 2019, **3**, 2326–2356.
33 C. Wang, C. Wang, L. Xu, H. Cheng, Q. Lin and C. Zhang, *Nanoscale*, 2014, **6**, 1775–1781.
34 Y.-S. Lin, Y.-F. Lin, A. Nain, Y.-F. Huang and H.-T. Chang, *Sens. Actuators Rep.*, 2021, **3**, 100026.
35 X. Yuan, Z. Luo, Y. Yu, Q. Yao and J. Xie, *Chem. – Asian J.*, 2013, **8**, 858–871.
36 J. Xie, Y. Zheng and J. Y. Ying, *J. Am. Chem. Soc.*, 2009, **131**, 888–889.
37 S. Govindaraju, S. R. Ankireddy, B. Viswanath, J. Kim and K. Yun, *Sci. Rep.*, 2017, **7**, 40298.
38 B. Hemmateenejad, F. Shakerizadeh-shirazi and F. Samari, *Sens. Actuators B Chem.*, 2014, **199**, 42–46.
39 J.-M. Liu, M.-L. Cui, S.-L. Jiang, X.-X. Wang, L.-P. Lin, L. Jiao, L.-H. Zhang and Z.-Y. Zheng, *Anal. Methods*, 2013, **5**, 3942–3947.
40 C.-Y. Lee, N.-Y. Hsu, M.-Y. Wu and Y.-W. Lin, *RSC Adv.*, 2016, **6**, 79020–79027.
41 R. Purohit and S. Singh, *Int. J. Nanomedicine*, 2018, **13**, 15–17.
42 B. A. Russell, B. Jachimska, I. Kralka, P. A. Mulheran and Y. Chen, *J. Mater. Chem. B*, 2016, **4**, 6876–6882.
43 M. Santhosh, S. R. Chinnadayyala, N. K. Singh and P. Goswami, *Bioelectrochemistry*, 2016, **111**, 7–14.
44 U. Anand, S. Ghosh and S. Mukherjee, *J. Phys. Chem. Lett.*, 2012, **3**, 3605–3609.
45 S. Ghosh, U. Anand and S. Mukherjee, *Anal. Chem.*, 2014, **86**, 3188–3194.
46 T. S. Sych, A. M. Polyanichko, L. V. Plotnikova and A. I. Kononov, *Anal. Methods*, 2019, **11**, 6153–6158.
47 W. Mi, S. Tang, Y. Jin and N. Shao, *ACS Appl. Nano Mater.*, 2021, **4**, 1586–1595.
48 T. Zhou, Y. Huang, W. Li, Z. Cai, F. Luo, C. J. Yang and X. Chen, *Nanoscale*, 2012, **4**, 5312–5315.
49 N. Goswami, A. Giri, M. S. Bootharaju, P. L. Xavier, T. Pradeep and S. K. Pal, *Anal. Chem.*, 2011, **83**, 9676–9680.
50 Y. Zhong, J. Zhu, Q. Wang, Y. He, Y. Ge and C. Song, *Microchim. Acta*, 2015, **182**, 909–915.
51 R. Rajamanikandan and M. Ilanchelian, *Mater. Sci. Eng. C Mater. Biol. Appl.*, 2019, **98**, 1064–1072.
52 S. Pandit and S. Kundu, *J. Lumin.*, 2020, **228**, 117607.
53 A. G. Thawari, P. Kumar, R. Srivastava and C. P. Rao, *Mater. Adv.*, 2020, **1**, 1439–1447.
54 S. Maity, D. Bain, S. Chakraborty, S. Kolay and A. Patra, *ACS Sustain. Chem. Eng.*, 2020, **8**, 18335–18344.
55 V. A. Proctor, F. E. Cunningham and D. Y. C. Fung, *C R C Crit. Rev. Food Sci. Nutr.*, 1988, **26**, 359–395.
56 E. D. N. S. Abeyrathne, H. Y. Lee and D. U. Ahn, *Poult. Sci.*, 2014, **93**, 1001–1009.
57 R. Diamond, *J. Mol. Biol.*, 1974, **82**, 371–391.
58 Y. An, Y. Ren, M. Bick, A. Dudek, E. Hong-Wang Waworuntu, J. Tang, J. Chen and B. Chang, *Biosens. Bioelectron.*, 2020, **154**, 112078.
59 C. Garza-Lombó, Y. Posadas, L. Quintanar, M. E. Gonsebatt and R. Franco, *Antioxid. Redox Signal.*, 2018, **28**, 1669–1703.
60 L. Wang, Y.-L. Yin, X.-Z. Liu, P. Shen, Y.-G. Zheng, X.-R. Lan, C.-B. Lu and J.-Z. Wang, *Transl. Neurodegener.*, 2020, **9**, 10.

61 M. Balali-Mood, K. Naseri, Z. Tahergorabi, M. R. Khazdair and M. Sadeghi, *Front. Pharmacol.*
62 E. L. Que, D. W. Domaille and C. J. Chang, *Chem. Rev.*, 2008, **108**, 1517–1549.
63 N. K. Das, S. Ghosh, A. Priya, S. Datta and S. Mukherjee, *J. Phys. Chem. C*, 2015, **119**, 24657–24664.
64 K. A. Weber, L. A. Achenbach and J. D. Coates, *Nat. Rev. Microbiol.*, 2006, **4**, 752–764.
65 H. Cao, Z. Chen, H. Zheng and Y. Huang, *Biosens. Bioelectron.*, 2014, **62**, 189–195.
66 N. Abbaspour, R. Hurrell and R. Kelishadi, *J. Res. Med. Sci. Off. J. Isfahan Univ. Med. Sci.*, 2014, **19**, 164–174.
67 U. Unicef and U. WHO, *Guide Programme Manag.*
68 J. L. Beard and J. R. Connor, *Annu. Rev. Nutr.*, 2003, **23**, 41–58.
69 T. Kassa, S. Jana, F. Meng and A. I. Alayash, *FEBS Open Bio*, 2016, **6**, 876–884.
70 V. Kumar, P. K. Bharti, M. Talwar, A. K. Tyagi and P. Kumar, *Water Sci.*, 2017, **31**, 44–51.
71 J. R. Lakowicz, *Principles of Fluorescence Spectroscopy*, Springer Science & Business Media, 2013.
72 S. R. Meech and D. Phillips, *J. Photochem.*, 1983, **23**, 193–217.
73 G. L. Long and J. D. Winefordner, *Anal. Chem.*, 1983, **55**, 712A-724A.
74 Daniel. MacDougall, W. B. Crummett and . et al., *Anal. Chem.*, 1980, **52**, 2242–2249.
75 J. Zheng, P. R. Nicovich and R. M. Dickson, *Annu. Rev. Phys. Chem.*, 2007, **58**, 409–431.
76 J. Zheng, C. Zhang and R. M. Dickson, *Phys. Rev. Lett.*, 2004, **93**, 077402.
77 C. Hariharan, V. Vijaysree and A. K. Mishra, *J. Lumin.*, 1997, **75**, 205–211.
78 A. O. El-Ballouli, E. Alarousu, A. R. Kirmani, A. Amassian, O. M. Bakr and O. F. Mohammed, *Adv. Funct. Mater.*, 2015, **25**, 7435–7441.
79 A. Pal, S. Srivastava, P. Saini, S. Raina, P. P. Ingole, R. Gupta and S. Sapra, *J. Phys. Chem. C*, 2015, **119**, 22690–22699.
80 S. Das, S. Rakshit and A. Datta, *J. Phys. Chem. C*, 2021, **125**, 15396–15404.
81 A. Akhuli, D. Chakraborty, A. K. Agrawal and M. Sarkar, *Langmuir*, 2021, **37**, 1823–1837.
82 K. A. Paterson, J. Arlt and A. C. Jones, *Methods Appl. Fluoresc.*, 2020, **8**, 025002.
83 A. I. Vogel, *Textbook of Macro and Semimicro Qualitative Inorganic Analysis*, Prentice Hall Press, London, 4th Revised edition., 1968.
84 H. Topal and Y. Topal, *Iran. Red Crescent Med. J.*, 2013, **15**, e12718.
85 K. K. Sahu, D. P. Dhibar, A. Gautam, Y. Kumar and S. C. Varma, *Turk. J. Emerg. Med.*, 2016, **16**, 119–120.
86 F. W. Bernhart and L. Skeggs, *J. Biol. Chem.*, 1943, **147**, 19–22.
87 J.-Y. Chang and L. Li, *FEBS Lett.*, 2002, **511**, 73–78.
88 R. Esquembre, J. M. Sanz, J. Gerard Wall, F. del Monte, C. Reyes Mateo and M. Luisa Ferrer, *Phys. Chem. Chem. Phys.*, 2013, **15**, 11248–11256.
89 V. A. Sirotkin and R. Winter, *J. Phys. Chem. B*, 2010, **114**, 16881–16886.